Vol. 13, No. 35, summer 2023, pages 63-77

Journal of Analytical and Numerical Methods in Mining Engineering

Journal home page: http://anm.yazd.ac.ir/

Research article

Numerical Modeling of Fluid Behavior on the Body of a Concrete Double-Arched Dam Considering the Interaction of Water and Structure under Impact Loads

Houman Rajabi[1], Babak Amin Nejad[2*], Hossein Ebrahimi[3]

1- Dept. of Civil Engineering, Kish International Branch, Islamic Azad University, Kish, Iran
2- Dept. of Civil Engineering, Roudehen Branch, Islamic Azad University, Tehran, Iran & Kish International Branch, Islamic Azad University, Kish, Iran
3- Dept. of Civil Engineering, Shahr-E-Qods Branch, Islamic Azad University, Tehran, Iran

*Corresponding author: E-mail: *babak_aminnejad1983@yahoo.com*
(Received: *July 2022*, Accepted: *June 2023)*

DOI: 10.22034/ANM.2023.18761.1561

Keywords

Impact
Double-arched concrete dam
Fluid
LBE
LS-DYNA

Abstract

One of the greatest issues regarding Iranian concrete dams is the lack of consideration for increasing our knowledge about them and their performance in times of accidents such as floods, earthquakes, and impact load caused by explosion waves. Some of the most significant objectives of this research are an investigation of the effect of TNT content and its distance from the concrete dam, the identification of critical points of the dam, and the impact of fluid on the amount of damage caused by the explosion to the concrete dam under impact load. The analysis used in this research is straightforward. It should be noted that the discovery of the critical points of the dam in the event of an accident, such as an explosion with complex behavior, can minimize human and financial losses. The LBE method was employed in this study. The interaction between the dam and the water behind it is one of the very considerable parameters that influence the deformation of the dam due to the hydrodynamic pressure of the water behind the dam. It is demonstrated by the results that doubling and tripling the amount of TNT leads to an increase in the pressure on the crest of the full dam by 46.63% and 64.68% respectively; besides, by multiplying the amount of TNT by four and five, the mentioned pressure increases by 70% and 75.58%, respectively.

1. INTRODUCTION

Some of the earliest studies on the interaction of the dam and the reservoir are the ones performed by Westergad to determine the hydrodynamic pressure on the rigid gravity dam, which has played a crucial role in the investigation of hydrodynamic force on the dam [1]. In 1952, Zangar developed a fast and simple method to calculate the hydrodynamic pressure on gravity dams regarding the slope of the upstream surface, in which fluid was assumed incompressible, the effect of surface waves was ignored and the hydrodynamic pressure was developed by the Laplace equation. From 1967 to 1981, Chopra et al. Conducted studies on the action and interaction between the dam, the reservoir, and its foundation.

Their results showed that rising water levels increase the risk in dams. Tian simulated the dynamic response of a concrete dam under load in an underwater explosion using LS-DYNA software, which results demonstrated that an explosion underwater is far more dangerous compared to one occurring on a dam or reservoir floor [2]. In 1966,

Reid presented a report on the response of the surface of a ship floating on the reservoir water under the influence of an underwater explosion. Due to the outbreak of World War II and its effects on military structures, the discussion of underwater explosions was seriously studied between 1941 and 1946 [3]. In 2009, Linsborough conducted a numerical study on a gravity dam with a crack in its upstream surface under the effect of seismic and impact loads, which main focus was on the investigation of the behavior of the dam with a crack under dynamic impact load. It was concluded that cracks created under impact loads are divided into three categories: closed, open, and stable, and open and unstable, which are created under the pressure of 5 MPa, 5-10 MPa, and more than 10 MPa, respectively.

In 2010, Ellis et al. examined the vulnerability of gravity concrete dams under the effects of explosions in an experimental manner and defined three types of material, local and structural failure [4]. In 2014, Wang et al. made use of a numerical simulation to predict the failure of a gravity concrete dam owing to an explosion underwater and reached a size of 100 mm mesh for the center of the explosion as the best size, and introduced four types of damages to the dam. Accordingly, it was observed that during the explosion, the amount of damage increased; finally, they presented a graph to express the relationship between the distance from the center of the explosion to the upstream of the dam, the number of explosives, and the conditions of destruction. Additionally, in a study on ship structure, they discovered that the ability of ABAQUS finite element methods to predict structural reactions, including fluid interactions, regarding the effect of bubble vibration, is confirmed and can have an acceptable presentation [5]. In 2016, Chen et al. Performed a numerical analysis of the gravity concrete dam under the explosion load and found that the presence of the overflow channel caused more damage to the upstream and upper part of the dam and the explosion in the middle of the overflow channel was more destructive than other points; consequently, As the depth of the explosion center increases, the damage to the dam can decrease [6].

Hirani et al. prepared another study on gravity concrete dams entitled "Seismic analysis of gravity concrete dams considering the dam-reservoir-foundation interaction", in which a nonlinear dynamic analysis of gravity concrete dams regarding the interaction effect of Dam-reservoir-foundation was performed. Bers examined the usage of Dyna finite element software to investigate explosion modeling. He analyzed his model at different depths and for different masses, then compared the results with the experimental ones. Fing et al. exposed the arched concrete dam to an initial shock caused by the underwater explosion; and then, using LS-DYNA software examined the displacements, velocity, and horizontal and vertical acceleration of the dam under the effect of the explosion shock and discovered that Horizontal responses are larger than vertical ones. In 2011, Nariman simulated the dynamic response of a concrete dam under the loading effect of an underwater explosion using LS-DYNA software. Sprago and Grace (2006) studied spectral element-finite element analysis of a ship-like structure that is exposed to underwater explosions. In this study of the fluid model, spectral elements with various degrees are utilized, and fluid cavitation models, as a nonlinear acoustic environment with a two-line bulk module are applied [7]. In 2007, Lacoli examined the shell of submerged cylinders filled with liquid exposed to shock waves and the impacts of structural-fluid interactions which focused on a number of acoustic and structural effects that occur during interaction. Lee et al. Studied the response of a floating structure under the effect of an underwater explosion considering the creation of volumetric cavitation. Other studies have been performed in which the impacts of an explosion on the interaction of solid and fluid environments have been investigated. Tech and Gabken analyzed the effects of water and flexible structure interaction during explosive loading and investigation of the effect of water-structure interactions and aerodynamic damping on the response of structures under explosive load is included in their research [8]. In 2009, Langerand et al. examined the integrity of a submarine body enduring an underwater explosive load. This paper deals with numerical methods for modeling and study of the resistance of submarine shells to the explosion, in which the phenomenon of structural-fluid interaction is also considered [9]. In 2014, Galedari et al. investigated the effect of standoff and charge weight on peak pressure and deformation of metallic plates subjected to underwater explosion [10]. Kalateh and Attarnejad (2011) studied the effects of acoustic cavitation and the resulting impact wave in the dynamic analysis of concrete dams. In this paper, a method for numerical analysis of acoustic cavitation in dam reservoirs and the resulting impact wave using the finite element method is presented [11]. In 2017, Chen analyzed the simulation of the damage mode of a gravity concrete dam in a close-in explosion, indicating that special attention ought to be paid to the concrete gravity dam that is exposed to shallow

underwater explosions close to the surface [12]. In 2017, Lu et al. evaluated an analytical response to the dynamic response of a dam through an underwater explosion. In addition, the vertical upstream surface and the sloping upstream surface in the two types of dams are investigated in this paper. The results indicated that the analytical solution can be applied to dams with vertical upstream surfaces [13]. In 2017, Moon et al. Conducted an experiment entitled "Assessment of the achievement of shock pressure driven by an underwater explosion" using measurement uncertainty. In the field of numerical analysis of the emission of impact waves, the methods of boundary element, finite element, finite difference, finite volume, and mesh-free are discussed. Pishevar and Amirifar performed the ALE method to simulate an underwater explosion and consequently, various underwater emissions were simulated [14]. In 2018, Chi Li studied the failure modes and analyzed the effects of gravity concrete dams with respect to the hydrostatic pressure caused by an underwater contact explosion which resulted that the initial hydrostatic pressure playing a significant role in the failure characteristics of the dam exposed to the underwater explosion. An underwater explosion in the deeper region can cause more serious damage to the heel of the dam and threaten the overall stability of the dam. Therefore, special attention should be paid to deep water explosions [15]. In 2018, Chi-ling Zhanga Duan performed numerical simulations of the nonlinear structural responses of an arch dam to an underwater explosion [16]. In 2018, Aminnejad et al. studied the impact of climate change on the inflow runoff to the Karun-4 dam, which indicated that under both B1 and RCP 2.6 modes, the annual input to the Karun-4 dam can be increased by 1.8% and 1.5%, respectively. Besides, under the two scenarios of A2 and RCP 8.5 modes, it decreases by 10.4% and 9.8%, respectively. The most significant objectives of the research are to investigate the effects of TNT content, its distance from the concrete dam, identification of critical points of the dam as well as fluid behind the dam, and the amount of damage caused by the explosion wave to the Concrete damn under explosion loading. In 2016, Aminnejad et al. reviewed the seismic performance evaluation of the Latian concrete dam by various records in order to investigate the reservoir effects using the finite element method. The most effective results of this research are the study of the main criteria of the damage to the upstream of the dam, modeling of reservoir damage, the behavior of gravity concrete dam against cracking, the performance of cantilever concrete dams due to the release of tensile stresses caused by vertical connections [17]. In 2014, Aminnejad et al. Studied the seismic performance of the Latian concrete dam (with different records) in order to investigate the reservoir effects using the finite element method whose most significant results are the main criteria of the damage to the upstream of the dam, modeling of reservoir damage, the behavior of gravity concrete dam against cracking and the performance of cantilever concrete dams due to the release of tensile stresses caused by vertical connections [18]. In 2014, they also investigated the parameters affecting the stability of gravity concrete dams with a case study in Folsom flat, blue rock dams to analyze the horizontal displacement related to the slip of the dam floor in contact with the foundation by ABAQUS software. By selecting three nodes at the bottom of the dam and similar nodes on the foundation and then by horizontally displacing these nodes relative to each other, the relative displacements of the dam were calculated; besides, it was observed that by increasing earthquake PGAs, the displacement diagram causes instability in dams [19].

In 2022, K. Zhang et al. studied the dynamic response of a gravity dam under air explosion load based on similarity law and in their comparison results of the models, they illustrated that there is a law of similarity between the dynamic response parameters of each scaling model obtained from simulation calculations and experimental fitting data, which is consistent with the theoretical results of the law of similarity. The method of expanding the dynamic parameters of the small-scale model to the large-scale model is reasonable and reliable [20].

In 2022, Mendomo Meye et al. conducted investigations on the dynamic response and failure mechanism of concrete arch dams under extreme loadings, the damage mechanism and characteristics of the dam under blast impact loads, as well as the evaluation of the condition of the dam after extreme loads [21].

In 2021, Razavi Toosi et al. investigated the effect of the explosion on the cyclic stresses and the created displacements on the body of the upper-ground cylindrical reinforced concrete water tank caused by hydrodynamic forces, taking into account the amount of water filling and the dimensions of the tanks with Abaqus software.

The results have indicated that the cyclic stresses of the body are affected by the explosion waves from the outside and the water pressure from the inside; accordingly, the presence of water

in the tank has caused the cyclic stresses in the body to increase by about 20 MPa [22].

In general, one of the greatest issues regarding Iranian concrete dams is the lack of consideration of increasing our knowledge about them and their performance in times of accidents such as floods, earthquakes, and especially explosions which can cause many human and financial losses.

Therefore, in this research, an attempt is made to evaluate the performance of the concrete dam after explosion loading at different distances and various amounts of TNT until reaching the rupture stage, regarding the interaction of water and the structure, as well as precisely investigation of the behavior and performance of the concrete dam and identification of critical and vulnerable points of the dam which can cause us severe damages in the time of the accident, so that we can minimize human and financial casualties in the time of accidents such as explosions whose behavior is complex.

Now, considering the importance of this issue, it is attempted to investigate the amount of damage caused by the explosion wave to the concrete dam with regard to the fluid behind it.

2. MATERIALS AND SOLUTION

2.1. Simulation

In order to validate this research, a simulation of investigation of the effect of water in the reservoir on the dynamic response of Karun-4 double-arched concrete dam under explosive loading in the open air was conducted by Kalateh et al., which was modeled by LS-DYNA software and its numerical results was compared to the mentioned simulation results. After a satisfactory agreement was reached between the numerical results of the simulation by Kalateh et al. and this research simulation results, then the simulation model of the Muropoint arch concrete dam under explosion is studied. In this research, the Karun-4 double-arched concrete dam with a height of 225 meters is numerically simulated [24]. An overview of the double-arched concrete dam is indicated in Fig 1.

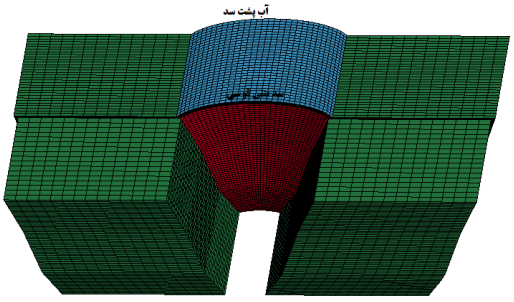

Fig. 1. An overview of the double-arched concrete dam.

2.2. Geometric Model

The SOLID element has 9 degrees of freedom, and in the three-dimensional space, it has eight nodes that are applied in explicit problems. An overview of the Solid element is shown in Fig 2.

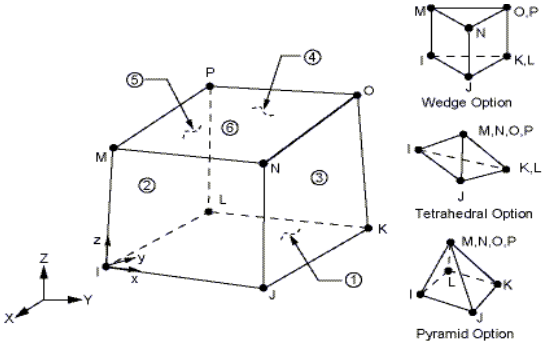

Fig. 2. Solid element geometric model.

In order to create a contact between the elements in this simulation, the command (CONSTRAINED_LAGRANGE_IN_SOLID) is made use of, which can make contact between the elements of two objects. Therefore, it is necessary to explain that all the floor nodes of the model are completely closed or in other words bound along the three axes.

2.3. Modeling Material Model

In this section, as it is known, an arched concrete dam is simulated considering the water behind the dam and the surrounding rocks against the explosion wave.

Therefore, in this part of the simulation, the MAT_JOHNSON_HOLMQUIST_CONCRETE material model is utilized to indicate the technical properties of concrete, the MAT_NULL model is used to show the technical characteristics of water, and the MAT_DRUCKER_PRAGER material model is applied to demonstrate the technical characteristics of rocks or soil around a double-arched concrete dam.

2.3.1. Concrete Material Model (Mat_Johnson_Holmquist_Concrete)

The Johnson Holmquist material model is applied in situations where concrete is subject to massive strains, severe strain changes, and high pressures. In this strength model, the concrete is defined as equivalent to a function of pressure, strain, and damage, and includes the effect of permanent deformation. Damage is described as a function of volumetric plastic strain, equivalent plastic strain, and pressure. Based on this model, the dimensionless equivalent stress is explained in the following equation.

In the above phrase, σ is the real equivalent stress and $f_c^{'}$ is the compressive strength. The value of σ^* for concrete is as follows.

$$\sigma^* = [A(1-D) + BP^{*N}][1 + C\ln \dot{\varepsilon}^*] \quad (1)$$

In the above relation, the parameter p^* represents the dimensionless pressure, which is defined as $p^* = \frac{p}{f_c'}$. ε^* is the dimensionless strain rate defined as $\dot{\varepsilon}^* = \frac{\dot{\varepsilon}}{\dot{\varepsilon}_\circ}$. The variable D represents the parameters of damage. ($0 \le D \le 1$). A is dimensionless adhesion strength, B is dimensionless compressive stiffness, N is the exponential stiffness and C is the strain rate coefficient of concrete. The considered damage to the element is as follows:

$$D = \sum \frac{\Delta\varepsilon P + \Delta\mu P}{D_1 (P^* + T^*)^{D_2}} \quad (2)$$

As observed above, $\Delta\mu P$ and $\Delta\varepsilon P$ indicate the increase of plastic strain and the increase of plastic volume strain, respectively; accordingly, D_1 and D_2 are the damage constants related to the material. Besides, T^* indicates the maximum dimensionless tensile stress, which is defined as $T^* = \frac{T}{f_c'}$. In this regard, T represents the maximum tensile stress. The relation described for the calculation of the pressure in the Johnson-Holmquist model, assuming that the material is dense, is indicated in the following relation.

$$P = \bar{\mu}K_1 + \bar{\mu}K_2 + \bar{\mu}K_3 \quad (3)$$

where, K_1, K_2, K_3 are constant values and $\bar{\mu}$ is the volume strain amount which is defined as follows:

$$\bar{\mu} = \frac{\mu - \mu_{lock}}{1 + \mu_{lock}} \quad (4)$$

In the above relation, μ_{lock} is the plastic volume strain [24].

The material model utilized for concrete in this section is MAT_JOHNSON_HOLMQUIST_CONCRETE; consequently, the model coefficients of the reinforcement material are represented in Table 1.

Table 1. Material model utilized for concrete [23,24]

Abbreviation	Concrete properties	Numerical values
R0	Density	2400 (kg/m^3)
G	Shear modulus	135670 (Mpa)
FC	Quasi-static uniaxial compressive strength	30 (Mpa)
A	Normalized cohesive strength	0.15
B	Normalized pressure hardening	0.15
N	Pressure hardening exponent	0.06
C	Strain rate coefficient	0.007
SFMAX	Normalized maximum strength	11.7
D1	Damage constant	0.03
D2	Damage constant	1
EFMIN	Amount of plastic strain before fracture	0.01
PC	Crushing pressure	(Mpa) 13.6
UC	Locking volumetric strain	0.00058
K1	Pressure constant	(Gpa) 17.4
K2	Pressure constant	38.8 (Gpa)
K3	Pressure constant	29.8 (Gpa)
PL	Locking pressure	(Mpa) 1.05
UL	Locking volumetric strain	0.1

2.3.2. The Material Model Of The Rocks Around Arched Concrete Dam

The material model considered in this simulation is number 193, version 970 of the software called MAT_DRUCKER_PRAGER. The numerical values of this material model are presented in Table (2).

Table 2. Material model applied for rocks around the arched concrete dam

Abbreviation	Water properties	Numerical values
R0	Density	(kg/m3) 2600
GMOD	Elastic Shear Modulus	(Mpa) 1400
RNU	Poisson Ratio	0.3
RKF	Failure Surface Shape Parameter	1
PHI	Angle of Friction	0.45
CVAK	Cohesion Value	0.766

2.3.3. Water Material Model

The material model considered in this simulation is called MAT_NULL, which has a state equation, and its numerical values are presented in Table (3). The equation of state for this material model is EOS_GRUNEISEN.

Table 3. The material model made use of water [23]

Abbreviation	Water properties	Numerical values
R0	MASS density	(kg/m3)1000
C	Speed of sound	1440 (m/s)
S1	Material constant	142
S2	Material constant	0.33
S3	Material constant	0.7
GAMAO	Material constant	0.5

2.3.4. Explosive model

In this research, the LOAD_BLAST_ENHANCED menu is used to load the blast in LS Dyna software.

Accordingly, the JWL equation of state and the MAT_HIGH_EXPLOSIVE_BURN material model is applied for the explosive model, whose pressure equation is defined as follows:

$$p = A\left[1-\frac{\omega}{R_1V}\right]e^{-R_1V_1} + B\left[1-\frac{\omega}{R_2V}\right]e^{-R_2V} + \frac{\omega E}{V} \quad (7)$$

where P is the pressure, R1, R2, B and A are coefficients that change based on the explosive material, V is the volume of the explosive material and E is the characteristic energy of the explosion.

Table 4. Specifications of the material model of explosives [21]

Abbreviation	Numerical values
(kg/m3) ρ	1.63
V_D (m/s)	6930
A (GPa)	374
B (GPa)	3/23
R_1	4/15
R_2	0/95
ω	0/38
V	1
E_0 (j/m^3)	6×10^9

2.4. Model Validation

The simulation of Kalateh et al. was performed by LS-Dyna software by changing the materials model and then the numerical results were compared to the results of the simulation. ANSYS and LS-DYNA software was applied for this simulation. Initially, the model was created in ANSYS software, and after meshing was entered in LS-DYNA software. The material model of MAT_JOHNSON_HOLMQUIST_CONCRETE was assigned to concrete (double-arched concrete dam) and material model of surrounding rocks was designated to material model number 193 of LS-DYNA software MAT_DRUCKER_PRAGER manual; accordingly, the water behind the dam was allocated to material model of MAT_NULL. Following to emission of the explosion wave from the explosive to the double-arched concrete dam, the pressure diagram applied to it was calculated. In this research, the explosive is a type of TNT, and the explosion load is located at a distance of 10 meters from the downstream surface of the dam body and at a height of 225 meters from the riverbed. The results obtained from the simulation of an arched concrete dam against an explosion wave can be observed in Figure (3).

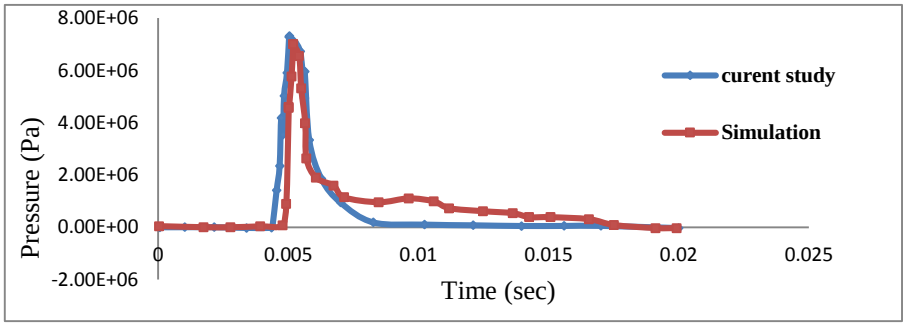

Fig. 3. Comparison of the simulation result with the simulation result of Kalateh et al.

The model under discussion is examined by Kalateh [24]. Based on the results of this simulation, the maximum pressure applied to the concrete dam is 7 MPa, the maximum pressure applied to the concrete dam in Kalateh research is 7.28 MPa and the difference is about 3.86%, which is an acceptable value for validation.

The amounts of 500, 1000, 1500, 2000, and 2500 kg of TNT in three states of full, half full, and empty in three coordinates of the crest of the dam, the middle of the dam, and the foot of the cantilever were simulated in LS Dyna software in order to investigate the damage caused by the blast wave to the arched concrete dam in the presented study.

3. RESULTS AND DISCUSSIONS

3. 1. Simulation In The Mode Of Empty Dam

At this point, the dam is emptied of water and the first stage of simulation, as TNT is at the crest of the dam, is the numerical simulation of 5 values of it. The results obtained from the dam, when it is empty, are analyzed in this section. In this research, it is planned to examine the dam in three states of empty of water, semi-full, and full of water in order to numerically evaluate the concrete dam against the load caused by the explosion wave on the dam body. Other effective variables are the position of TNT at three different heights of the concrete dam and its values; consequently, its position was numerically simulated for each stage of modeling at three different heights, once at the foot of the dam cantilever (bottom of the dam), in the middle of the dam height, and finally at the dam crest site for 5 TNT values.

The numerical results of the maximum pressure applied to the concrete dam, as the TNT is located at the crest of the dam, are demonstrated in Table (5). As observed in the results, by doubling the mass of TNT, the maximum pressure applied to the crest of the dam, which is emptied of water, increases by 46%. By tripling the mass of TNT, it reaches about 64% and by quadrupling it the maximum pressure applied to the dam increases by about 70%. In addition, by multiplying its mass by five, this amount rises by up to 75%.

Table 5. Numerical results caused by the maximum pressure applied to the concrete dam

TNT mass (kg)	Maximum pressure applied to the crest of the empty dam (MPa)	Maximum pressure applied to the middle of the empty dam (MPa)	Maximum pressure applied to the foot of the empty dam cantilever (MPa)
500	1.257	1.453	1.789
1000	2.320	2.515	3.550
1500	3.550	3.717	5.814
2000	4.137	4.584	6.848
2500	5.031	5.227	8.218

Besides, by doubling the amount of TNT, the maximum pressure applied to the crest of the dam, which is emptied of water, increases by 46%. By tripling the amount of TNT, it reaches about 61% and by quadrupling it the maximum pressure applied to the dam increases by about 69%. In addition, by multiplying its amount by five, this amount rises up to 73%.

Numerical results of the maximum pressure applied to the concrete dam in the case where the position of TNT is at the base of the dam cantilever, indicate that by doubling the mass of TNT, the maximum pressure applied to the crest of the dam, which is emptied of water, increases by 50%. By tripling its mass, this amount is increases by about 70%. By quadrupling the TNT mass, the maximum pressure applied to the dam increases by about 74%, and by multiplying its amount by five, this amount rises up to 78%.

3.2. Simulation In Semi-Full Dam State

In this state, the water behind the dam is considered semi-full and the study is performed in 5 different cases where the amount of TNT is from 500 kg to 2500 kg and the dam is under the effect of the explosion waves.

In this part of the dissertation, the numerical study of the concrete dam against the load caused by the explosion wave of the dam in a semi-full state is considered. One of the effective variables is the position of TNT at three different heights of the concrete dam and its amount. TNT position was numerically simulated for each stage of modeling as an empty and semi-full dam at three different heights, which are at the base of the dam cantilever (at the bottom of the dam), in the middle of the dam height, and finally at the crest of the dam for 5 different values of TNT. The

numerical results of the TNT explosion wave at the dam crest are indicated in Table (6).

Table 6. Numerical results of TNT explosion wave in the dam crest

TNT mass (kg)	Maximum pressure applied to the semi-full dam (MPa)	Maximum pressure applied to the empty dam (MPa)	Difference *(%)*
500	1.928	1.257	34.8%
1000	3.605	2.320	36%
1500	5.674	3.550	37%
2000	6.624	4.137	38%
2500	7.882	5.031	36%

Consequently, the maximum pressure applied to the concrete dam in different positions of TNT (empty dam) is presented in Figure (4). the numerical results of the maximum pressure applied to the concrete dam when the TNT position is at the dam crest are presented in Table (6). As observed from the results, by doubling the amount of TNT, the maximum pressure applied to the dam, which is emptied of water, in the crest of the dam increases by 47%; by tripling it, this amount reaches about 66%. Additionally, by quadrupling its mass, the maximum pressure applied to the dam increases by about 71%, and finally by multiplying it by five, this amount increases by up to 76%.

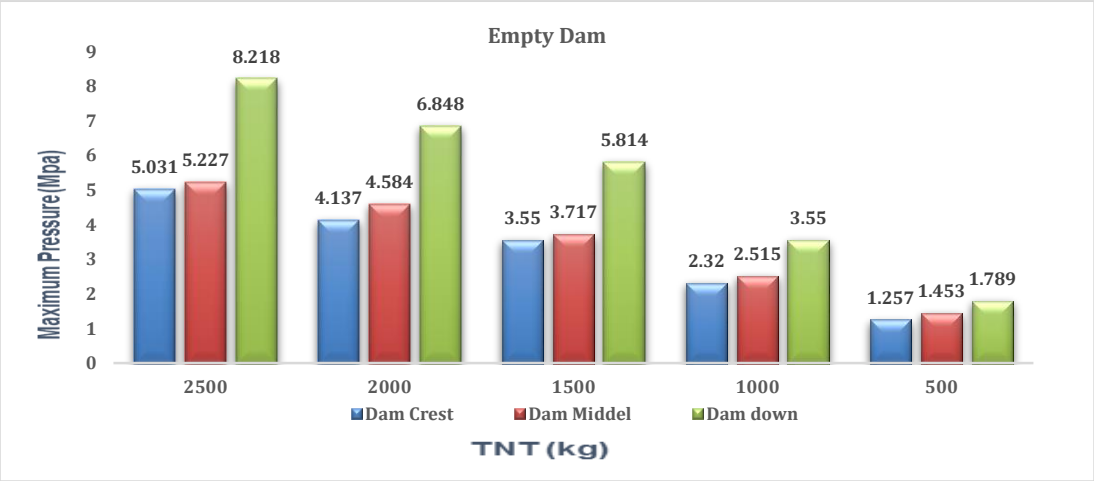

Fig. 4. Maximum pressure applied to the concrete dam considering different positions of TNT (dam is emptied of water).

Table 7. Numerical results of the TNT explosion wave in the middle of the dam

TNT mass (kg)	Maximum pressure applied to the semi-full dam (MPa)	Maximum pressure applied to the empty dam (MPa)	Difference *(%)*
500	2.068	1.453	30%
1000	4.025	2.515	38%
1500	5.925	3.717	37.5%
2000	7.379	4.584	38%
2500	8.553	5.227	39%

The results demonstrated in Table (7) are due to the maximum pressure applied to the concrete dam when the TNT position is located in the middle of the dam. As observed, the dam is considered both empty and semi-full; and accordingly, the maximum pressure applied to the concrete dam due to the explosion wave indicates the values of TNT from 500 kg to 2500 kg, which is in Mpa. The highest pressure is when the amount of TNT is 2500 kg and the dam is semi-full of water, also the lowest pressure is applied when the amount of TNT is 500 kg and the dam is empty of water. The numerical results of the maximum pressure applied to the concrete dam when the TNT position is in the middle of the dam are illustrated in Table (7), which indicates that by

doubling the amount of TNT, the maximum pressure applied to the empty dam, in its middle, increases by 49%. By tripling it, this amount increases by about 65%. In addition, by quadrupling the TNT mass, the maximum pressure applied to the dam increases by about 72%, and finally by multiplying it by five, it reaches 76%.

The numerical results of the maximum pressure applied to the concrete dam in the case where TNT is at the base of the dam cantilever are demonstrated in Table (8). As observed, most of the pressure is applied to the dam when it is semi-full of water. The numerical results caused by the maximum pressure applied to the concrete dam when the TNT is at the bottom of the dam are indicated in Table (7). As observed, by doubling the amount of TNT, the maximum pressure applied to the dam, which is emptied of water, at the bottom of it increases by 42%. By tripling it, this amount increases by about 65%; besides, by quadrupling its mass, the maximum pressure applied to the dam increases by about 70%, and finally by multiplying it by five, this amount increases up to 75%.

Table8. Numerical results of the TNT explosion wave at the bottom of the dam

TNT mass (kg)	Maximum pressure applied to the semi-full dam (MPa)	Maximum pressure applied to the empty dam (MPa)	Difference *(%)*
500	2.431	1.789	26%
1000	4.192	3.55	15%
1500	6.848	5.814	16%
2000	8.050	6.848	16%
2500	9.699	8.218	15%

3.3. Simulation In the State Of a Fully Water-Filled Dam

In this section, a numerical study of the concrete dam against the load caused by the explosion wave in three states of empty of water, semi- full and full of water is performed. Some of the most effective variables of this article are to be noted: the presence of fluid behind the dam, the position of TNT at three different heights of the concrete dam, and the amount of TNT in different coordinates. TNT position was numerically investigated in each stage of modeling as an empty, semi-full, and full dam, at three different heights being the base of the dam cantilever (bottom of the dam), its middle height, and at its crest, for 5 values of TNT in two modes of with and without-fluid. The numerical results obtained from the simulation are summarized in Table 9.

The maximum pressure applied to the concrete dam when TNT is located at its crest in three states of full, half full, and empty of water are presented in Table 9.

Table 9. Numerical results of TNT explosion wave in the dam crest

TNT mass (kg)	Full dam (MPa)	Semi-full dam (MPa)	Empty dam (MPa)
500	2.655	1.928	1.257
1000	4.975	3.605	2.320
1500	7.519	5.674	3.550
2000	8.860	6.624	4.137
2500	10.874	7.882	5.031

The amounts of mentioned pressure for a mass of 500 kg TNT in three states of the full, semi-full, and empty dam are 2.655, 1.928, and 1.257 MPa, respectively. These values are obtained at 4.975, 3.605, and 2.320 MPa for the mass of 1000 kg, respectively. Accordingly, for the mass of 1500 kg, they obtained 7.519, 5.674, and 3.550 MPa, respectively. They are also acquired 8.860, 6.624, and 4.137 MPa, for the mass of 2000 kg and 10.874, 7.882, and 5.031 MPa for the mass of 2500 kg, respectively.

As indicated in the results, by doubling the amount of TNT, the pressure applied to the crest of a full dam increases by 46.63% and reaches 64.68% by tripling it. besides, by multiplying the amount of TNT by four and five, the pressure experiences a 70% and 75.58% increase, respectively. As observed, most of the pressure is applied to the dam when the dam is full of water.

The maximum pressure applied to the concrete dam when TNT is located in the middle of the dam crest in three states of full, semi-full, and empty is demonstrated in Table (10). The amounts of pressure applied to the middle of the concrete dam in the empty, semi-full, and full state for the mass of 500 kg of TNT are 2.739, 2.068, and 1.453 MPa, respectively. Consequently, for a mass of 1000 kg, these values are obtained at 5.227, 4.025, and 2.515 MPa, respectively. In addition, the pressure amounts applied to the middle of the dam in the three different conditions, for a mass of 1500 kg TNT, are estimated at 7.770, 5.925, and 3.717, respectively; and they are 9.671, 8.553, and

5.227, for the mass of 2000 kg, and accordingly 11.97, 8.553 and 5.227 for the mass of 2500 kg, respectively. It is indicated by obtained results that by doubling the amount of TNT, the pressure applied to the middle of the dam when the dam is full, increases by 47.60% and reaches 64.74% by tripling its amount. Besides, by multiplying it by four and five, the pressure experiences a 71.67% and 75.31% increase, respectively. As observed, the maximum pressure is applied in the condition where the dam is full of water.

Results also demonstrate that by doubling the amount of TNT, the pressure applied to the middle of the dam, when the dam is semi-full, increases by 48.62% and reaches 65.1% by tripling its amount. Additionally, by multiplying it by four and five, the pressure experiences a 72% and 75.82% increase, respectively.

Table 10. Numerical results of the TNT explosion wave in the middle of the dam

TNT (kg)	Full dam (MPa)	Semi-full dam (MPa)	Empty dam (MPa)
500	2.739	2.068	1.453
1000	5.227	4.025	2.515
1500	7.770	5.925	3.717
2000	9.671	7.379	4.584
2500	11.097	8.553	5.227

The maximum pressure applied to the concrete dam when TNT is located at its foot in three states of full, half full, and empty of water are presented in Table 11.

Table 11. Numerical results of the TNT explosion wave at the foot of the dam cantilever

TNT mass (kg)	full dam (MPa)	Semi-full dam (MPa)	Empty dam (MPa)
500	3.130	2.431	1.789
1000	6.652	4.192	3.550
1500	11.013	6.848	5.814
2000	12.942	8.050	6.848
2500	13.559	9.699	8.218

The amounts of pressure applied to the bottom of the concrete dam in the empty, semi-full, and full state for the mass of 500 kg of TNT are 3.130, 2.431, and 1.789 MPa, respectively. Accordingly, for a mass of 1000 kg, they obtained 6.652, 4.192, and 3.550 MPa, respectively. Besides, the pressure amounts applied to the bottom of the dam in the three different conditions, for a mass of 1500 kg TNT, are acquired at 11.013, 6.848, and 5.814, respectively; and they are 12.942, 8.050, and 6.848 for the mass of 2000 kg, and consequently 13.599, 9.699 and 8.218 for the mass of 2500 kg, respectively. As obtained by results, by doubling the amount of TNT, the pressure applied to the foot of the cantilever of the full dam increases by 52.60% and reaches 71.60% by tripling its amount. Besides, by multiplying it by four and five, the pressure experiences a 75.8% and 77% increase, respectively. Results also indicate that by doubling the amount of TNT, the pressure applied to the foot of the cantilever of the semi-full dam increases by 42% and reaches 64.5% by tripling its amount. Besides, by multiplying it by four and five, the pressure experiences 69.81% and 74.93% increase, respectively.

The maximum pressure applied to the concrete dam in the position where the TNT is located at its crest is indicated in Figure (5). It is observed in the results that by doubling the amount of TNT, the pressure applied to the dam crest, when the dam is semi-full, increases by 47% and reaches 65% by tripling its amount. Consequently, by multiplying it by four and five, the pressure experiences 70% and 75.5% increase, respectively. Generally, it is obvious that the lowest amount of pressure is applied when the dam is empty and TNT is at its lowest level. In other words, less pressure is applied when the dam is empty compared to the semi-full and full states. It is demonstrated by obtained results that by doubling the amount of TNT, the pressure applied to the dam crest, when the dam is empty, increases by 45.81% and reaches 64.6% by tripling its amount. Consequently, by multiplying it by four and five, the pressure experiences a 69.61% and 75% increase, respectively.

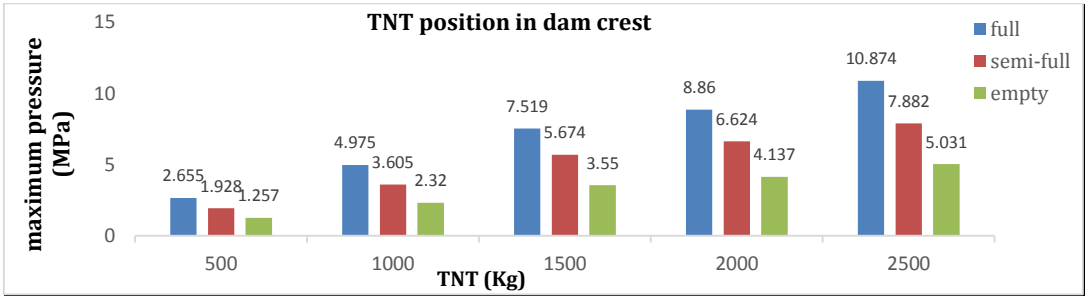

Fig. 5. Comparison of the maximum pressure applied to the crest of the concrete dam in three states of empty, full, and semi-full.

The results obtained from different amounts of TNT, from 500 kg to 2500 kg, when it is located in the middle of the dam are presented according to Figure (6). As observed, the maximum pressure is applied when the amount of TNT is 2500 kg and the dam is full of water. In other words, more pressure is applied to the semi-full dam comparing to the empty one. Additionally, by doubling and tripling the amount of TNT, the pressure applied to the middle of the empty dam increases by 42.22% and 61%, respectively. Consequently, by multiplying it by four and five, the pressure experiences 68.30% and 72.22% increase, respectively.

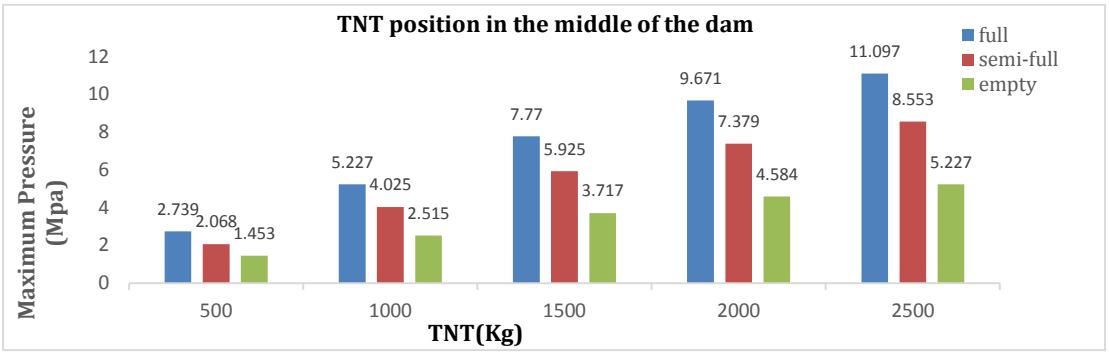

Fig. 6. Comparison of the maximum pressure applied to the middle of the concrete dam in three states of empty, full, and semi-full.

The maximum pressure applied to the concrete dam in the position where the TNT is located at the foot of the dam cantilever is illustrated in Figure (7). It is observed that by doubling the amount of TNT, the pressure applied to the foot of dam cantilever, when dam is empty, increases by 49.60% and reaches 69.22% by tripling its amount. Consequently, by multiplying it by four and five, the pressure experiences 73.87% and 78% increase, respectively.

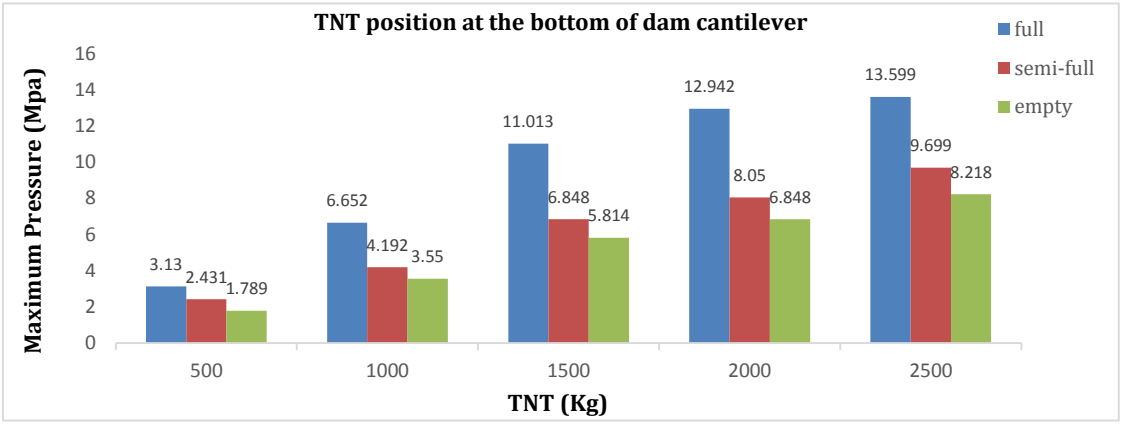

Fig. 7. Comparison of the maximum pressure applied to the concrete dam at the foot of its cantilever in three states of empty, full, and semi-full.

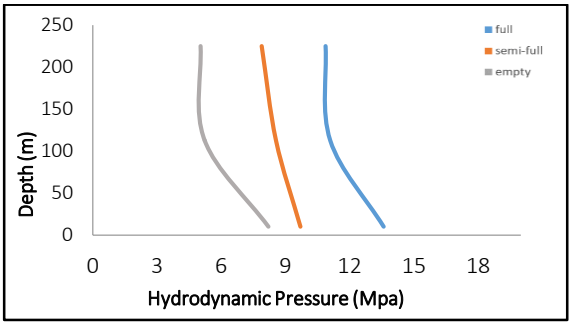

Fig. 8. Diagram of the depth of the posterior water of the dam according to the pressure applied to the concrete dam (crest of the dam: 225 meters high, middle of the dam: 1125.5 meters, and the foot of the dam console: 10 meters from the floor).

As indicated in Figure 8, the amount of hydrodynamic pressure applied to the foot of the dam console for a mass of 2500 kg in three states of full, half full, and empty is 13.59, 9.69, and 8.20 MPa respectively. This value is obtained at 11.09, 8.55, and 5.22 MPa, respectively, for the state of the water depth up to the middle of the dam. Also, the pressure applied to the crest of the dam for a mass of 2500 kg is acquired as 10.8, 7.88, and 5.03 MPa, respectively.

In general, with the occurrence of the explosion and the increase in the posterior hydrodynamic pressure of the dam, near the explosion site (near the body of the dam), it

reaches its maximum state and then the pressure is distributed throughout the entire body of the concrete dam. The results demonstrate that the dynamic pressure atteined from the foot of the dam cantilever is higher than its other parts.

Besides, the most critical state of this research is when the dam is full of water and the hydrodynamic pressure at the foot of the dam console reaches its highest value. The distribution of the wave caused by the explosion at different time steps to the body of the double-arched concrete dam at different heights are shown in Figure 9.

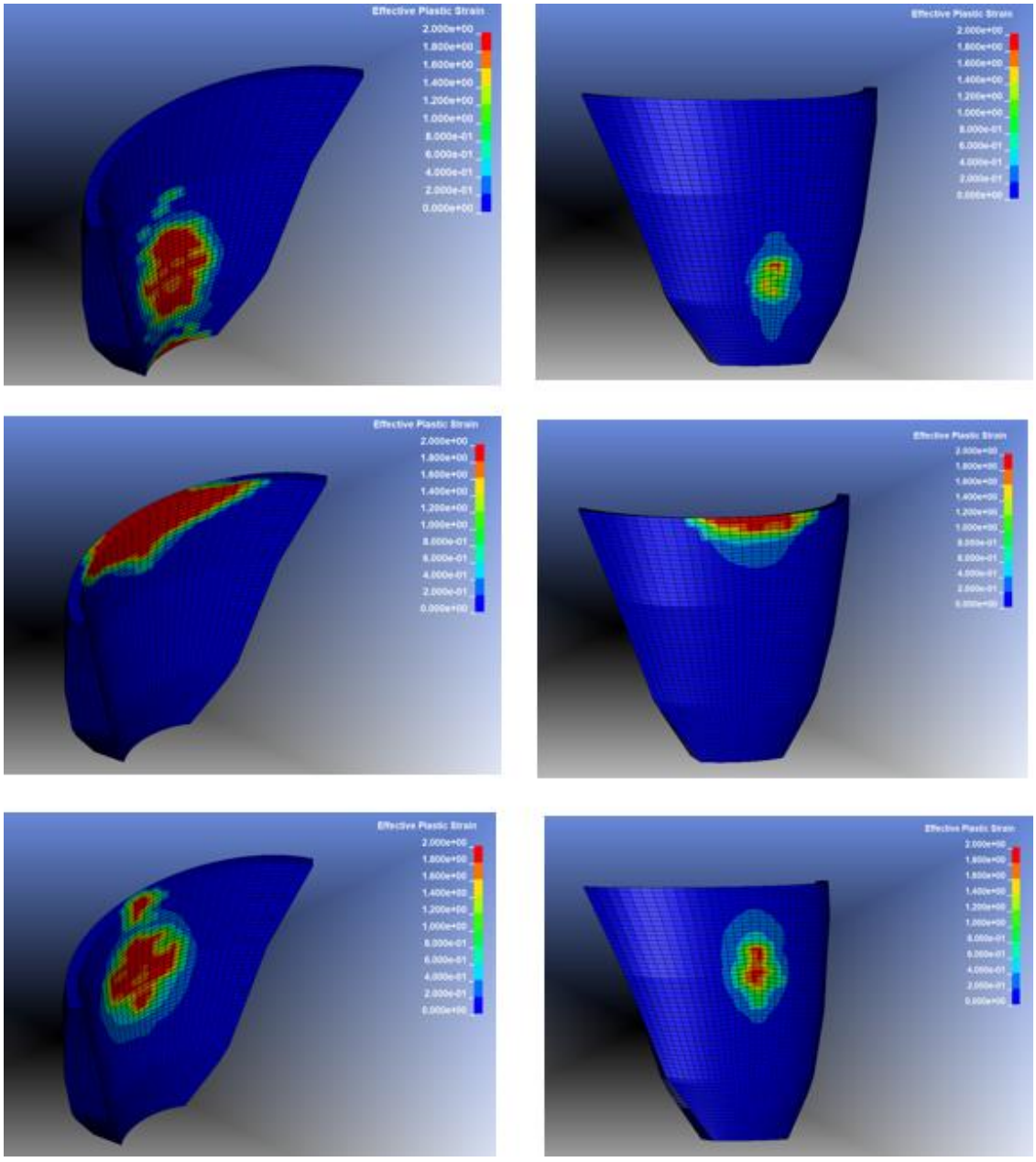

Fig. 9. Schematic of the emission of the wave caused by the explosion to the body of the double-arched concrete dam at different heights.

4. CONCLUSIONS

This research aims the study the damage caused by the explosion wave to the double-arched concrete dam with respect to the fluid behind the dam. The values of 500, 1000, 1500, 2000, and 2500 kg of TNT in three states of the full, semi-full, and empty dam, in three coordinates of the dam crest, the middle of the dam and the foot of its cantilever are simulated in the software; besides, the maximum pressure applied to the double-arched concrete dam is investigated in the mentioned cases and the most effective results obtained in this research are as follows:

1. By doubling the amount of TNT, the maximum pressure applied to the crest of the empty dam increases by 47%. By tripling it, this amount increases by about 66%. In addition, by quadrupling its mass, the maximum pressure reaches about 71%, and finally, by multiplying it by five, it increases by up to 76%.

2. By doubling the amount of TNT, the maximum pressure applied to the middle of the empty dam increases by 49%. By tripling it, this amount increases by about 65%. In addition, by quadrupling its mass, the maximum pressure reaches about 72%, and finally, by multiplying it by five, it increases up to 76%.

3. By doubling the amount of TNT, the maximum pressure applied to the foot of the empty dam increases by 42%. By tripling it, this amount increases by about 65%. In addition, by quadrupling its mass, the maximum pressure reaches about 70%, and finally, by multiplying it by five, it increases up to 75%.

4. As indicated in the results, the lowest applied pressure at the dam crest, is when the TNT value is the lowest and is equal to 1.257 MPa and the dam is empty of water. In other words, when the dam is empty, the applied pressure has the lowest value, while in the case of a semi-full dam, the pressure from the fluid behind the dam and the explosion wave act in the same way, and consequently, this puts more pressure on the concrete dam.

5. According to the results of this research, the lowest applied pressure at the bottom of the dam is when the amount of TNT is the lowest and is equal to 1.789 MPa and the dam is empty of water. However, compared to this state, more pressure is applied to a semi-full dam. In general, the wave caused by the explosion and the pressure caused by the fluid behind the dam act in the same way, which causes more pressure to be applied to the concrete dam compared to the case where the dam is empty of water.

6. Results show that the amount of maximum pressure applied to the crest of the empty dam for a mass of 500 kg of TNT is obtained at 1.257 MPa and is 1.928 in the case of the semi-full dam which is increased by 34.80% compared to an empty dam. However, the applied amounts of pressure to an empty and semi-full dam are obtained at 2.320 and 3.605 MPa for a mass of 1000 kg, respectively. Comparing the empty dam mode to the semi-full one, the mentioned pressure is increased by 36%. Accordingly, for masses of 1500, 2000, and 2500 kg, this amount is associated with an average increase of 37%.

7. As indicated by results, the amount of maximum pressure applied to the middle of the empty dam for a mass of 500 kg of TNT is obtained at 1.453 MPa and is 2.068 in the case of the semi-full dam which is increased by 30% compared to an empty dam. In addition, the applied pressure to an empty and semi-full dam is obtained at 2.515 and 4.025 MPa for the mass of 1000 kg, respectively. Comparing the empty dam mode to the semi-full one, the mentioned pressure is increased by 38%. Consequently, for masses of 1500, 2000, and 2500 kg, this amount is associated with an average increase of 38.2%.

8. As observed in the results, by doubling the amount of TNT, the maximum pressure applied to the crest of the full dam increases by 46.63%. By tripling it, this amount increases by about 64.68%. In addition, by multiplying it by four and five, it increases by 70% and 75%, respectively. As seen, the maximum pressure applied is when the dam is fully filled with water.

9. It is demonstrated by results that by doubling the amount of TNT in the condition of a full dam, the maximum pressure applied to the middle of it increases by 47.60%. By tripling it, this amount increases by about 64.74%. In addition, by multiplying it by four and five, it increases by 71.67% and 75.31%, respectively. As observed, the maximum pressure applied is when the dam is fully filled with water.

10. Results indicate that by doubling the amount of TNT, the maximum pressure applied to the middle of a semi-full dam increases by 48.62%. By tripling it, this amount increases by about 65.1%. In addition, by multiplying it by four and five, it increases by 72% and 75.82%, respectively.

11. Results show that by doubling the amount of TNT in the condition of a full dam, the maximum pressure applied to the foot of its cantilever increases by 52.60%. By tripling it, this amount increases by about 71.60%. In addition, by multiplying it by four and five, it increases by 75.8% and 77%, respectively.

12. It is indicated by results that by doubling the amount of TNT, the maximum pressure applied to the foot of the dam cantilever, which is semi-full, increases by 42%. By tripling it, this amount increases by about 64.5%. In addition, by multiplying it by four and five, it increases by 69.81% and 74.93%, respectively.

13. As demonstrated by the results, by doubling the amount of TNT, the maximum pressure applied to the foot of the cantilever of the empty dam increases by 49.60%. By tripling it, this amount increases by about 69.22%. In addition, by multiplying it by four and five, it increases by 73.87% and 78%, respectively.

14. It seems that the two prominent factors that cause the difference in the behavior of the bottom, middle, and top of the dam in the three states of empty, half full, and full, can be pointed out as the hardness of different parts of the concrete dam as well as the increase in the amount of explosive load to reach the rupture time in the direction of the foot of the dam console rather than its other parts. In other words, due to the fact that the foot of the dam console is harder than other parts of the dam, it is identified as the most critical area which experiences the most pressure.

15. With the occurrence of the explosion and the increase of the hydrodynamic pressure behind the dam near the explosion spot (near the body of the dam), the pressure reaches its maximum state and after the explosion, the pressure is distributed throughout the body. As observed in the results, the dynamic pressure attained from the foot of the dam cantilever is higher than its other parts.

16. It is demonstrated by results that the highest dynamic pressure occurred at the foot of the dam console regarding the location of the explosion, which can be a threat to the instability of the concrete dam.

17. The distribution of dynamic pressure starts with the initiation of the explosion at the closest point to its place, and as time goes by, distributes throughout the entire body.

18. Generally, the presence of fluid behind the dam has an increasing impact on the response of the structure against the explosion according to the place of the explosion loading (near the body of the dam and in its inner part). Consequently, the amount of dynamic pressure has also increased considering the interaction of water and structure.

19. The most critical state of this research is when the dam is full of water and the hydrodynamic pressure at the foot of the dam console has reached its highest value

20. The reason for the increase in explosive load to reach the rupture time in the direction of the foot of the dam console compared to other parts of the dam is the greater hardness of this area compared to the middle of the dam and its crest.

REFERENCES

[1] Westergaard, Harold Malcolm. "Water pressures on dams during earthquakes." Transactions of the American society of Civil Engineers 98, no. 2 (1933): 418-433.

[2] Zangar, Carl Nicholas. Hydrodynamic pressures on dams due to horizontal earthquake effects. No. 11. Technical Information Office, 1952.

[3] Reid, Warren D. The Response of Surface Ships to Underwater Explosions. Defence Science and Technology organization canberra (AUSTRALIA), 1996.

[4] Linsbauer, Herbert. "Hazard potential of zones of weakness in gravity dams under impact loading conditions." Frontiers of Architecture and Civil Engineering in China 5, no. 1 (2011): 90-97.

[5] Wang, Hao, Xi Zhu, Yuan Sheng Cheng, and Jun Liu. "Experimental and numerical investigation of ship structure subjected to close-in underwater shock wave and following gas bubble pulse." Marine Structures 39 (2014): 90-117.

[6] Chen, J., Liu, X., and Xu, Q., 2016, Numerical simulation analysis of damage mode of concrete gravity damunder close-in explosion, KSCE Journal of Civil Engineering; 21(1):397–407.

[7] Nariman,A., "Parametric Analysis of Dam-Reservoir Interaction Subject to Shock Wave Due to

Underwater Explosion." M.sc Thesis, Malek Ashtar University of Technology 2011(In Persian).

[8] Iakovlev, S. "Submerged fluid-filled cylindrical shell subjected to a shock wave: fluid–structure interaction effects." Journal of fluids and structures 23, no. 1 (2007): 117-142.

[9] Langrand, Bertrand, Nicolas Leconte, Aude Menegazzi, and Thierry Millot. "Submarine hull integrity under blast loading." International journal of impact engineering 36, no. 8 (2009): 1070-1078.

[10] Galehdari, S. A., H. Khodarahmi, S. Hadidi Moud, and A. Karimi. "Analysis of Stand Off and Charge Weight Effect on Peak Pressure and Deformation of Metallic Plate Subjected to Under Water Explosion." Advanced Defense Science and Technology 3 (2014): 207-216.

[11] Nourouzi, Fardin, Farhoud Kalateh, and Mohammad Ali Lotfollahi-Yaghin. "Numerical Analysis of Dynamic Response of Concrete Gravity Dam under Blast Loading in the Reservoir." Journal of Civil and Environmental Engineering 47, no. 86 (2017): 91-104.

[12] Chen, Jianyun, Xiaopeng Liu, and Qiang Xu. "Numerical simulation analysis of damage mode of concrete gravity dam under close-in explosion." KSCE Journal of Civil Engineering 21, no. 1 (2017): 397-407.

[13] Lu, Lu, Degao Zou, Ye Zhu, Yun Dong, Chunyuan Zuo, and Yachao Wu. "An analytical solution for dynamic response of water barrier subjected to strong shock waves caused by an underwater explosion to dams." Polish Maritime Research 24, no. S2 (94) (2017): 111-117.

[14] Pishevar, A. R., and R. Amirifar. "An adaptive ALE method for underwater explosion simulations including cavitation." Shock Waves 20, no. 5 (2010): 425-439.

[15] Li, Qi, Gaohui Wang, Wenbo Lu, Xinqiang Niu, Ming Chen, and Peng Yan. "Failure modes and effect analysis of concrete gravity dams subjected to underwater contact explosion considering the hydrostatic pressure." Engineering Failure Analysis 85 (2018): 62-76.

[16] Zhang, Qi-Ling, Duan-You Li, Fan Wang, and Bo Li. "Numerical simulation of nonlinear structural responses of an arch dam to an underwater explosion." Engineering Failure Analysis 91 (2018): 72-91.

[17] Mansouri, A., B. Aminnejad, and H. Ahmadi. "Investigating the effect of climate change on inflow runoff into the Karun-4 Dam based on IPCC's fourth and fifth report." JWSS-Isfahan University of Technology 22, no. 2 (2018): 345-359.

[18] Movahedi, N. Salman, and B. Aminnejad. "Seismic performance assessment of latyan concrete buttress dam subjected to different records including reservior effects by finite element method." Journal of Fundamental and Applied Sciences 8, no. 3 (2016): 1206-1220.

[19] behradimehr, E. mansouri, and B. Aminnejad. "Folsom, Blue Stone. "The Investigation of Effective Parameters on the Stability of Concrete Gravity Dams with Case Study on Folsom, Blue Stone, and Pine Flat Dams". American Journal of Civil Engineering and Architecture.2014. 2(5):167-173.

[20] K. Zhang, F. Lu, Y. Peng, and X. Li, "Study on dynamic response of gravity dam under air blast load based on similarity law," Eng. Fail. Anal, (2022): vol. 138, p. 106225.

[21] S. Mendomo Meye, G. Li, Z. Shen, J. Zhang, G. F. Emani, and V. Edem Setordjie, "Dynamic Response and Failure Mechanism of Concrete Arch Dams under Extreme Loadings: A Solid Foundation for Real-World Actions to Reduce Dam Collapse Losses during Wartime or Terrorist Attacks," Water J., (2022): vol. 14, no. 10, p. 1648.

[22] V. Razavi Tusi, M. Moghadam, M. Shahrbanouzadeh "Dynamic analysis of reinforced concrete water tanks under explosion with regard to water-structure interaction" Scientific Journal of Passive Defense. (2021).

[23] KALATEH, F., H. GHANBARI, and Ravan A. Roshan. "Investigation of Water Level in the Reservoir on Dynamic Response of Karun IV Arch Dam under Air Blast Loading." (2018): 17-26.

[24] FUKUSHIMA, Satoshi, Koushi KUMAGAI, Tsuyoshi YASUKI, and Yoshiharu SONODA. "LS-DYNA Version 970 User's Manual LS-DYNA Version 970 User's Manual, 2005."